


Single ionization of an asymmetric diatomic system by relativistic charged projectilesA. Jacob, C. Müller, and A. B. Voitkiv *Institut für Theoretische Physik I, Heinrich Heine Universität Düsseldorf, Universitätsstr. 1, 40225 Düsseldorf, Germany*

(Received 2 February 2021; accepted 19 March 2021; published 5 April 2021)

We study single ionization of a heteroatomic system by charged projectiles whose velocity v approaches the speed of light c . The system is formed by two loosely bound atomic species, A and B , with the ionization potential of A being smaller than excitation energy for a dipole-allowed transition in B . In such a case, three single ionization channels occur: (i) single-center ionization of atom A , (ii) single-center ionization of atom B , and (iii) two-center ionization of A . While (i) and (ii) are the well known mechanism of direct impact ionization of a single atom, in channel (iii) ionization of A proceeds via impact excitation of B with consequent radiationless transfer of excitation energy—via (long-range) two-center electron-electron correlations—to A , leading to its ionization. We show that, close to the resonance energy, the two-center channel (iii) is so enormously strong that its contribution remains dominant even if the range of emission energies ~ 1 eV, which is orders of magnitude broader than its width, is considered. The influence of relativistic effects, caused by a high collision velocity, on the angular distribution of emitted electrons may be quite strong even at $\gamma = 1/\sqrt{1 - v^2/c^2} \approx 2$. However, in the energy distribution and the total cross section, these effects become substantial only at $\gamma \gg 1$. Relativistic effects arising due to a large size of the two-atomic system are shown to be very weak even for a ${}^7\text{Li-He}$ dimer whose mean size is about 28 Å.

DOI: [10.1103/PhysRevA.103.042804](https://doi.org/10.1103/PhysRevA.103.042804)**I. INTRODUCTION**

Ionization occurring in ion-atom collisions belongs to the basic phenomena studied by atomic physics. The direct impact ionization of an atom by a charged projectile (e.g., an electron, an ion) is a well-known process which has been studied for a wide range of collision energies including relativistic ones (see, e.g., Refs. [1–3] and references therein).

In this paper, we consider single ionization of a loosely bound heteroatomic system bombarded by relativistic bare ions. The system consists of two atomic species A and B , which are separated by a distance much larger than the typical atomic size, and it is assumed that the ionization potential of A is smaller than an excitation energy of a dipole-allowed transition in B .

Under such conditions single ionization of the A - B system can proceed via three basic channels: (i) direct (single) ionization of A , (ii) direct ionization of B , and (iii) two-center ionization of A . While the channels (i) and (ii) represent the well-known process of single ionization of a single atom, the channel (iii) is a more subtle ionization mechanism in which correlations between electrons belonging to the different atomic centers play the crucial role. This mechanism involves impact excitation of a dipole-allowed transition in B with the subsequent radiationless decay of the excited state of B via long-range two-center electron-electron correlations which transmit the de-excitation energy to atom A that results in its ionization.

One has to mention that two-center electron correlations may cause a variety of other interesting phenomena. For instance, they drive the population inversion in a He-Ne laser

and the energy transfer in quantum optical ensembles [4] or cold Rydberg gases [5]. They are also crucial for Förster resonances between chromophores [6] in biological systems. Another two-center phenomenon is represented by interatomic Coulombic decay (ICD) [7] in which the electronic excitation energy of one of the atoms cannot be quickly released through a forbidden (single-center) Auger decay and is instead transferred to the neighboring atom resulting in its ionization. Processes based on correlated electronic decay have been also found in expanding nanoplasmas which were formed by irradiating clusters with intense laser pulses [8].

Inter-atomic electron-electron correlations are also responsible for the process of resonant two-center photoionization (2CPI) [9] in which ionization of a Van der Waals dimer occurs via resonant photoabsorption by one of its atoms with subsequent interatomic coulombic decay. It was experimentally observed in Ne-He dimers [10,11] and large NeAr clusters [12]. The process that is time inverse of two-center photoionization is termed two-center dielectronic recombination (2CDR) [13]. Here, an incident electron is captured by an ion via resonant transfer of the energy excess to the neighbor atom which afterwards stabilizes via spontaneous radiative decay. If the energy excess is larger than the ionization potential of the neighbor atom, electron emission from this atom takes place. This process is called interatomic coulombic electron capture (ICEC) [14].

Recently, the process of two-center ionization in nonrelativistic collisions with electrons was studied in [15]. The present paper, where ionization of a large-size asymmetric dimer by high-energy ions is considered, focuses on the role of relativistic effects in this process which are caused by both

a collision velocity approaching the speed of light and a large size of the dimer.

The paper is organized as follows. In Sec. II, we consider single-electron emission from the A - B system and derive differential and total cross sections for all emission channels, where we especially focus on two-center ionization. Section III contains numerical results and discussion. Finally, our main findings are summarized in Sec. IV. Atomic units ($\hbar = |e| = m_e = 1$) are used throughout unless otherwise stated.

II. THEORETICAL CONSIDERATION

A. General approach

Let us consider a diatomic system consisting of two weakly bound atomic species A and B which are in their ground states with energies ε_g and ε_e , respectively. We suppose that B has an excited state with an energy ε_e , which can be populated by a dipole-allowed transition from the ground state of B , and that the excitation energy of this transition in B is larger than the ionization potential I_A of A : $\omega_B = \varepsilon_e - \varepsilon_g > I_A$.

We also assume that the nuclei of A and B are separated by the internuclear distance R which is much larger than the typical atomic size such that the electron orbitals of A and B essentially do not overlap and, besides, the interaction between A and B is relatively weak. Then, the electronic structure of the A - B system may be approximately considered as that of two individual noninteracting species A and B .

Let now the A - B system be bombarded by a bare ion P with the charge Z_P and (relative) velocity v . In the present consideration, we shall assume that the projectile has a relatively low charge, i.e., that the condition $Z_P/v \ll 1$ is fulfilled. Under such a condition the projectile field will represent just a weak perturbation for the A - B system and we may use the first order of (time dependent) perturbation theory in order to treat the interaction between this system and the projectile. Besides, this condition also implies that (total) ionization of the A - B system will be largely dominated by single ionization processes.

As was already mentioned, in collisions with charged projectiles there are two direct (one-step) and one indirect (two-step) ionization channels which lead to single ionization of the A - B system. The two direct channels are the single-center impact ionization of either atom A or B . The indirect channel—which we term two-center impact ionization—is of two-center nature involving both atomic species and can be subdivided into two steps.

In the first step, the interaction between the projectile P and atom B leads to a dipole allowed transition from the ground state of B with energy ε_g into its excited state with energy ε_e . Afterwards, B radiationlessly decays into its initial ground state with the energy release being transferred—via the (long-range) two-center electron-electron interaction—to A . As a result of the energy transfer atom A undergoes a transition from its ground state with energy ε_g into a continuum state with energy ε_k . A scheme of two-center ionization is shown in Fig. 1(a).

As is already rather obvious, two-center impact ionization (unlike the direct ionization) is a resonant process which occurs within a very narrow range of electron emission energies

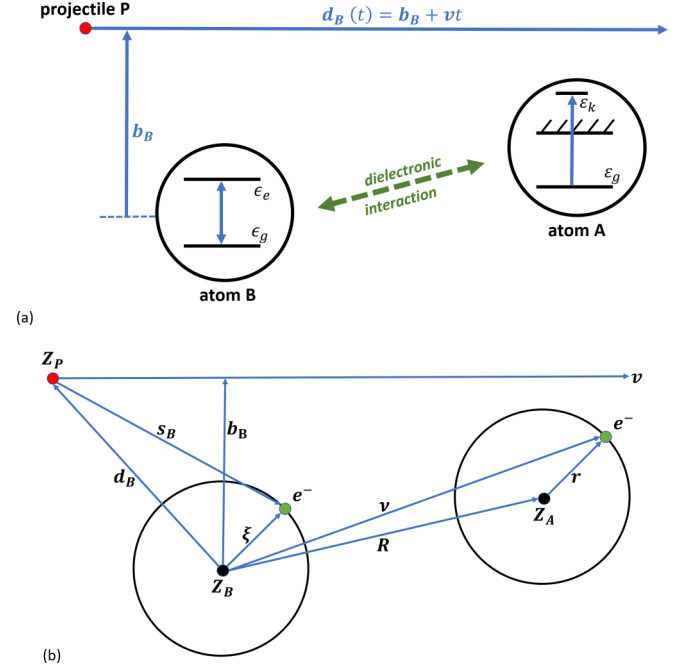


FIG. 1. (a) Scheme of two-center ion impact ionization and (b) schematic representation of space coordinates characterizing the collision.

centered around the resonance energy $\varepsilon_{k,r} = (\varepsilon_e - \varepsilon_g) + \varepsilon_g \equiv \omega_B - I_A$. We shall see, however, that despite the energy interval affected by this channel being tiny, it is so enormously strong on the resonance and close to it that its presence may noticeably influence even the total cross section.

Before we proceed further, two remarks may be appropriate. First, the condition $\varepsilon_e - \varepsilon_g > I_A$ ensures that we only have to deal with two-center ionization of A and not B . Second, in our present treatment of all ionization channels, we shall consider only one ‘active’ electron in each atom A and B .

Our treatment of collisions between the A - B system and the projectile will be based on the semi-classical approximation in which the relative motion of the heavy particles (nuclei) is treated classically while the ‘active’ electrons are considered quantum mechanically. Note that this approximation is very well justified for high energy collisions [1].

We choose a reference frame in which the A - B system is at rest and take the nucleus of B as the origin. Let $\mathbf{r}(\xi)$ be the coordinate of the single active electron in A (B) with respect to the nucleus of A (B). Further, let \mathbf{R} be the internuclear vector between A and B .

In this reference frame, the projectile P moves along a classical straight-line trajectory $\mathbf{d}_B(t) = \mathbf{b}_B + \mathbf{v}t$, where $\mathbf{b}_B = (b_x, b_y, 0)$ is the impact parameter in the B - P collision and $\mathbf{v} = (0, 0, v)$ the collision velocity. Further, $\mathbf{s}_B(t) = \xi - \mathbf{d}_B(t)$ is the distance vector between the active electron in B and the ion P . The corresponding coordinates for the A - P collision can be obtained by simple vector addition. The collision geometry for two-center ionization is illustrated in Fig. 1(b).

It is well-known (see, e.g., Ref. [16]), that the main contribution to the total ionization cross section is given by emission energies not greatly exceeding the initial electron binding energy. Therefore we may use the nonrelativistic Schrödinger

equation

$$i \frac{\partial \Psi(t)}{\partial t} = \hat{H} \Psi(t) \quad (1)$$

to describe the motion of the active electrons. In (1), the Hamiltonian \hat{H} reads

$$\hat{H} = \hat{H}_A + \hat{H}_B + \hat{V}_{AB} + \hat{W}_A + \hat{W}_B. \quad (2)$$

Here, \hat{H}_A (\hat{H}_B) is the Hamiltonian for free atom A (B), \hat{V}_{AB} is the interaction between A and B , and \hat{W}_A (\hat{W}_B) is the interaction between the projectile and atom A (B).

The interaction \hat{V}_{AB} , which at relatively large interatomic distances R is mainly of the dipole-dipole character, can be derived by considering the coupling $j_\mu^A A_B^\mu$ between the transition four-current j_μ^A of the electron in atom A and the four-potential A_B^μ of the field created by the electron of atom B (or vice versa). A detailed derivation of \hat{V}_{AB} is given in Appendix A and the corresponding result reads

$$\hat{V}_{AB} = e^{iR\frac{\omega_A}{c}} \left[\left(\mathbf{r} \cdot \boldsymbol{\xi} - \frac{3(\mathbf{r} \cdot \mathbf{R})(\boldsymbol{\xi} \cdot \mathbf{R})}{R^2} \right) \frac{1 - iR\frac{\omega_A}{c}}{R^3} - \left(\mathbf{r} \cdot \boldsymbol{\xi} - \frac{(\mathbf{r} \cdot \mathbf{R})(\boldsymbol{\xi} \cdot \mathbf{R})}{R^2} \right) \frac{\left(\frac{\omega_A}{c}\right)^2}{R} \right], \quad (3)$$

where c is the speed of light and $\omega_A = \varepsilon_k - \varepsilon_g$ is the transition energy in A . In the limit of comparatively small interatomic distances, $R \ll c/\omega_A$, equation (3) takes on the well known form of the instantaneous interaction between two electric dipoles

$$\hat{V}_{AB} = \left(\mathbf{r} \cdot \boldsymbol{\xi} - \frac{3(\mathbf{r} \cdot \mathbf{R})(\boldsymbol{\xi} \cdot \mathbf{R})}{R^2} \right) \frac{1}{R^3}, \quad (4)$$

which scales with the distance as R^{-3} . Expression (3), in particular, takes into account that the electromagnetic field, which transmits the interaction between the atoms, propagates with the finite velocity ($= c$) that leads to the so called retardation effect. As it follows from the form of (3), this effect becomes important for interatomic distances $R \gtrsim c/\omega_A$ changing the R dependence of \hat{V}_{AB} from $\sim R^{-3}$ at $R \ll c/\omega_A$ to $\sim R^{-1}$ at $R \gg c/\omega_A$. Thus, in our case of resonant two-center transitions, the account of relativistic effects in the interatomic interaction results in a substantial increase of its range. This could be contrasted with the case when two atoms are in the ground state, where relativistic effects reduce the interaction range changing the R -dependence of the van der Waals potential from $\sim R^{-6}$ to $\sim R^{-7}$.

Let us now consider the interaction \hat{W}_j ($j = A, B$) between the projectile and atom j . Taking into account that the electron motion is nonrelativistic this interaction can be written as

$$\hat{W}_j = \frac{1}{2c} [\hat{\mathbf{p}}_j \cdot \mathbf{A}_j + \mathbf{A}_j \cdot \hat{\mathbf{p}}_j] - \phi_j + \frac{1}{2c^2} \mathbf{A}_j^2 + \frac{1}{2c} \boldsymbol{\sigma} \cdot \mathbf{B}_j, \quad (5)$$

where $\hat{\mathbf{p}}_j$ ($\hat{\mathbf{p}}_A = \hat{\mathbf{p}}_r$, $\hat{\mathbf{p}}_B = \hat{\mathbf{p}}_\xi$) is the momentum operator for the 'active' electron in atom j . Further, ϕ_j and \mathbf{A}_j are the scalar and vector potential, respectively, which describe the field of the projectile ion acting on the active electron in j . We shall take these potentials in the Liénert-Wiechard form in

which they read (see, e.g., Ref. [17])

$$\phi_j = \frac{\gamma Z_P}{|s'_j(t)|}, \quad \mathbf{A}_j = \frac{\mathbf{v}}{c} \phi_j, \quad (6)$$

where γ is the Lorentz factor and

$$s'_A(t) = (\mathbf{r}_\perp - \mathbf{b}_A - \mathbf{R}_\perp, \gamma(r_\parallel - R_\parallel - vt)), \\ s'_B(t) = (\boldsymbol{\xi}_\perp - \mathbf{b}_B, \gamma(\xi_\parallel - vt)). \quad (7)$$

Here, \mathbf{r}_\perp (r_\parallel), $\boldsymbol{\xi}_\perp$ (ξ_\parallel) and \mathbf{R}_\perp (R_\parallel) are the transverse (longitudinal) parts of the coordinates \mathbf{r} , $\boldsymbol{\xi}$ and \mathbf{R} which are perpendicular (parallel) to the collision velocity \mathbf{v} . Note that the potentials in (6) satisfy the Lorentz condition $\partial_\mu A_j^\mu = 0$ for the four-potential $A_j^\mu = (\phi_j, \mathbf{A}_j)$.

Finally, in (5) $\boldsymbol{\sigma}$ are the Pauli matrices and \mathbf{B}_j is the magnetic field of the projectile which acts on the active electron in j . From the theory of single-center impact ionization, it is known (see, e.g., Ref. [18]) that spin effects are negligible for light atomic targets and accordingly we drop the interaction term $\frac{1}{2c} \boldsymbol{\sigma} \cdot \mathbf{B}_j$ in our calculation.

The consideration of the interaction term proportional to A_j^2 in (5) requires especial care. In Ref. [16], it was shown that in a self-consistent first order treatment one has to omit the $1/(2c^2) A_j^2$ term in the Schrödinger equation and so do we.

The initial state Ψ_{gg} of the A - B system reads

$$\Psi_{gg}(\boldsymbol{\xi}, \mathbf{v}, t) = \phi_g(\mathbf{v} - \mathbf{R}) e^{-i\varepsilon_g t} \chi_g(\boldsymbol{\xi}) e^{-i\varepsilon_g t}, \quad (8)$$

where ϕ_g (χ_g) is the ground state of atom A (B) and $\mathbf{v} = \mathbf{R} + \mathbf{r}$. Considering single-center impact ionization of atom A , the final state Ψ_{kg} is given by

$$\Psi_{kg}(\boldsymbol{\xi}, \mathbf{v}, t) = \phi_k(\mathbf{v} - \mathbf{R}) e^{-i\varepsilon_k t} \chi_g(\boldsymbol{\xi}) e^{-i\varepsilon_g t}. \quad (9)$$

Here, ϕ_k is the continuum state of the electron ejected from A with an asymptotic momentum \mathbf{k} . Similarly, the final state Ψ_{gk} for single-center ionization of atom B is determined by

$$\Psi_{gk}(\boldsymbol{\xi}, \mathbf{v}, t) = \phi_g(\mathbf{v} - \mathbf{R}) e^{-i\varepsilon_g t} \chi_k(\boldsymbol{\xi}) e^{-i\varepsilon_k t}, \quad (10)$$

where χ_k is the continuum state of the electron emitted from B with an asymptotic momentum \mathbf{k} .

Concerning two-center impact ionization of A , in addition to the initial state (8) and the final state (9), we must also take into account the intermediate state(s)

$$\Psi_{ge}(\boldsymbol{\xi}, \mathbf{v}, t) = \phi_g(\mathbf{v} - \mathbf{R}) e^{-i\varepsilon_g t} \chi_e(\boldsymbol{\xi}) e^{-i\varepsilon_e t} \quad (11)$$

with χ_e the excited state of B .

B. Transition amplitudes

The channels for single-center and two-center ionization of atom A interfere with each other since they both lead to the same final state of the A - B system. Accordingly, the transition amplitude for the ionization of atom A consists of the direct amplitude $S_{1C}^A(\mathbf{b}_A)$ and two-center amplitude $S_{2C}(\mathbf{b}_B)$ and reads

$$S_{1C+2C}(\mathbf{b}_A, \mathbf{b}_B) = S_{1C}^A(\mathbf{b}_A) + S_{2C}(\mathbf{b}_B). \quad (12)$$

The channel for single-center ionization of atom B leads to electron emission from B instead of A and, hence, does not interfere with the other two channels.

1. Amplitude for ionization of atom A

Using the first order of time dependent perturbation theory, the transition amplitude S_{1C}^A in (12) is defined by

$$S_{1C}^A(\mathbf{b}_A) = \frac{1}{i} \int_{-\infty}^{\infty} dt \langle \phi_k | \hat{W}_A(\mathbf{b}_A, t) | \phi_g \rangle e^{i\omega_A t}, \quad (13)$$

where the interaction \hat{W}_A between A and the projectile P is given by (5).

Actually, it is more convenient to consider the amplitude (13) in momentum space. The corresponding Fourier transform to momentum space and its inverse are given by

$$\begin{aligned} \tilde{S}(\mathbf{q}_\perp) &= \frac{1}{2\pi} \int d^2\mathbf{b} S(\mathbf{b}) e^{i\mathbf{q}_\perp \cdot \mathbf{b}}, \\ S(\mathbf{b}) &= \frac{1}{2\pi} \int d^2\mathbf{q}_\perp \tilde{S}(\mathbf{q}_\perp) e^{-i\mathbf{q}_\perp \cdot \mathbf{b}}, \end{aligned} \quad (14)$$

where \mathbf{q}_\perp has the meaning of the perpendicular part of the momentum transfer between the projectile and the A-B system in the collision.

Using (13) and the first equation in (14) we obtain that the amplitude $\tilde{S}_{1C}^A(\mathbf{q}_\perp)$ for the direct ionization of A in the momentum space reads

$$\tilde{S}_{1C}^A(\mathbf{q}_\perp) = \frac{2Z_P}{ivq^2} \mathcal{F}_{k_g}^{\Delta m}(\mathbf{q}) e^{i\mathbf{q} \cdot \mathbf{R}}. \quad (15)$$

Here,

$$\mathcal{F}_{k_g}^{\Delta m}(\mathbf{q}) = \langle \phi_k | e^{i\mathbf{q} \cdot \mathbf{r}} \left[\frac{\mathbf{v} \cdot \hat{\mathbf{p}}_r}{c^2} + \frac{\omega_A}{2c^2} - 1 \right] | \phi_g \rangle \quad (16)$$

and

$$\begin{aligned} \mathbf{q} &= \left(\mathbf{q}_\perp, \frac{\omega_A}{v} \right), \\ \mathbf{q}' &= \left(\mathbf{q}_\perp, \frac{\omega_A}{\gamma v} \right). \end{aligned} \quad (17)$$

In (17), \mathbf{q} and \mathbf{q}' are the momentum transfer from the projectile to the target A as viewed in the rest frame of the target and projectile, respectively.

In order to obtain the amplitude for two-center ionization of atom A, we need to use the second order of perturbation theory where both the interaction of the projectile with atom B and the interatomic interaction \hat{V}_{AB} are present. Then the corresponding transition amplitude S_{2C} in (12) for two-center ionization is obtained to be

$$S_{2C}(\mathbf{b}_B) = \sum_{\Delta m=-1}^1 S_{2C}^{\Delta m}(\mathbf{b}_B). \quad (18)$$

Here, $\Delta m = 0, \pm 1$ denotes the change in the magnetic quantum number for the dipole-allowed excitation transition in B and

$$S_{2C}^{\Delta m}(\mathbf{b}_B) = \frac{1}{i^2} \int_{-\infty}^{\infty} dt \mathcal{M}_2^{\Delta m}(t) \int_{-\infty}^t dt' \mathcal{M}_1^{\Delta m}(\mathbf{b}_B, t'), \quad (19)$$

where $\mathcal{M}_1^{\Delta m}(\mathbf{b}_B, t') = \langle \Psi_{ge} | \hat{W}_B(\mathbf{b}_B, t') | \Psi_{gg} \rangle$ and $\mathcal{M}_2^{\Delta m}(t) = \langle \Psi_{kg} | \hat{V}_{AB} | \Psi_{ge} \rangle$. Substituting the states from (8), (9) and (11)

into (19) yields

$$\begin{aligned} S_{2C}^{\Delta m}(\mathbf{b}_B) &= \frac{1}{i^2} \int_{-\infty}^{\infty} dt \mathcal{M}_{AB}^{\Delta m} e^{i(\omega_A - \omega_B)t} \\ &\quad \times \int_{-\infty}^t dt' \mathcal{M}_B^{\Delta m}(\mathbf{b}_B, t') e^{i\omega_B t'}, \end{aligned} \quad (20)$$

where $\mathcal{M}_{AB}^{\Delta m} = \langle \phi_k \chi_g | \hat{V}_{AB} | \phi_g \chi_e \rangle$ is the interatomic matrix element which describes the de-excitation in atom B and the ionization of atom A and $\mathcal{M}_B^{\Delta m} = \langle \chi_e | \hat{W}_B | \chi_g \rangle$ the matrix element for the impact excitation of B. Defining $F(t) = \int_{-\infty}^t dt' \mathcal{M}_B^{\Delta m}(\mathbf{b}_B, t') e^{i\omega_B t'}$, the transition amplitude in (20) becomes

$$S_{2C}^{\Delta m}(\mathbf{b}_B) = \frac{1}{i^2} \int_{-\infty}^{\infty} dt \mathcal{M}_{AB}^{\Delta m} e^{i(\omega_A - \omega_B)t} F(t). \quad (21)$$

The interatomic matrix element $\mathcal{M}_{AB}^{\Delta m}$ is constant for finite t and vanishes at the boundaries $t = \pm\infty$ (this corresponds to the assumption that the interaction between A and B is adiabatically switched on and off at $t \rightarrow -\infty$ and $t \rightarrow +\infty$, respectively). Taking this into account, we can perform in (21) integration by parts that yields

$$S_{2C}^{\Delta m}(\mathbf{b}_B) = \frac{-i\mathcal{M}_{AB}^{\Delta m}}{\delta + i\frac{\gamma}{2}} \int_{-\infty}^{\infty} dt \mathcal{M}_B^{\Delta m}(\mathbf{b}_B, t) e^{i\omega_A t}. \quad (22)$$

Here, $\delta = \omega_A - \omega_B$ and the appearance of γ ($\gamma \rightarrow +0$) reflects the assumption about adiabatic switching the interaction on and off at $|t| \rightarrow \infty$ according to $\sim \exp(-\gamma|t|/2)$.

A more careful treatment of two-center ionization (which includes also the channel of spontaneous radiative decay of the excited state of B and goes beyond the 'standard' perturbative theory) shows that the infinitesimally small parameter γ in (22) should be replaced by the finite total width $\Gamma^{\Delta m}$ of the intermediate state (11) accounting for the finite lifetime of this state. The total width is the sum, $\Gamma^{\Delta m} = \Gamma_r^B + \Gamma_a^{\Delta m}$, of the radiative width,

$$\Gamma_r^B = \frac{4\omega_B^3}{3c^3} |\langle \chi_e | \hat{\xi} | \chi_g \rangle|^2, \quad (23)$$

due to the spontaneous radiative decay of the excited state χ_e and the two-center autoionization width,

$$\Gamma_a^{\Delta m} = \frac{k_r}{(2\pi)^2} \int d\Omega_k |\mathcal{M}_{AB}^{\Delta m}(k_r)|^2, \quad (24)$$

where $k_r = \sqrt{2(\omega_B - I_A)}$ is the resonant value for the momentum of the emitted electron and Ω_k is the solid angle for electron emission, which arises due to the nonradiative decay of the excited state χ_e caused by the two-center electron-electron interaction.

As before, it is more convenient to work with the two-center ionization amplitude written in momentum space which is obtained by applying the Fourier transformation (14) to the amplitude (22), which yields

$$\tilde{S}_{2C}(\mathbf{q}_\perp) = \frac{2Z_P}{ivq^2} \sum_{\Delta m=-1}^1 \frac{\mathcal{M}_{AB}^{\Delta m} \mathcal{F}_{eg}^{\Delta m}(\mathbf{q})}{\delta + i\Gamma^{\Delta m}/2} \quad (25)$$

with

$$\mathcal{F}_{eg}^{\Delta m}(\mathbf{q}) = \langle \chi_e | e^{i\mathbf{q} \cdot \hat{\mathbf{p}}_\xi} \left[\frac{\mathbf{v} \cdot \hat{\mathbf{p}}_\xi}{c^2} + \frac{\omega_A}{2c^2} - 1 \right] | \chi_g \rangle. \quad (26)$$

2. Amplitude for ionization of atom B

Similarly to the consideration of direct ionization of atom A, we obtain that the transition amplitude \tilde{S}_{1C}^B for the direct ionization of atom B reads

$$\tilde{S}_{1C}^B(\mathbf{q}_\perp) = \frac{2Z_P}{ivq_B^2} \mathcal{F}_{\kappa_g}^{\Delta m}(\mathbf{q}_B). \quad (27)$$

Here,

$$\mathcal{F}_{\kappa_g}^{\Delta m}(\mathbf{q}_B) = \langle \chi_\kappa | e^{i\mathbf{q}_B \cdot \boldsymbol{\xi}} \left[\frac{\mathbf{v} \cdot \hat{\mathbf{p}}_\xi}{c^2} + \frac{\omega_B^{\text{ion}}}{2c^2} - 1 \right] | \chi_{g'} \rangle, \quad (28)$$

where κ is the asymptotic momentum of the emitted electron, $\omega_B^{\text{ion}} = \epsilon_\kappa - \epsilon_g$ the transition energy for the bound-continuum transition in B with ϵ_κ being the energy of the continuum state. The momenta \mathbf{q}_B and \mathbf{q}'_B transferred in the collision resulting in ionization of atom B are given by

$$\begin{aligned} \mathbf{q}_B &= (\mathbf{q}_\perp, \omega_B^{\text{ion}}/v), \\ \mathbf{q}'_B &= (\mathbf{q}_\perp, \omega_B^{\text{ion}}/(\gamma v)) \end{aligned} \quad (29)$$

(as viewed in the rest frame of the target and projectile, respectively).

3. Ionization of atom B and the A^+-B system

In the presence of atom A, the ion-impact ionization of atom B can trigger a further development in the residual $A-B^+$ system resulting in the same electronic final state as the direct and two-center ionization of atom A considered in subsection II B 1.

Indeed, the B^+ ion, formed due the ion-impact ionization, will polarize atom A that leads to the appearance of an attractive interatomic force. When the two atomic centers approach sufficiently close each other, an outer electron of atom A can be transferred to the ion B^+ via radiative capture mechanism. In such a case, one has the neutral atom B (in the ground state) and the ion A^+ .

The above mentioned process involves the interaction between two atomic centers and, in this sense, can be viewed as a kind of two-center ionization which might noticeably increase the number of collision events resulting in the appearance of the A^+-B system (but at the expense of those where $A-B^+$ system would be formed). However, unlike the two-center ionization process considered in subsection II B 1, this process is not resonant with the shape of the electron emission spectrum being similar to that of the ion-impact ionization of a single atom B and it will not be considered here.

C. Cross sections

1. Cross sections for ionization of atom A

The spectrum of electrons emitted from atom A is determined by the cross section differential in the electron momentum

$$\frac{d^3\sigma_{1C+2C}}{dk^3} = \int d^2\mathbf{q}_\perp |\tilde{S}_{1C}^A(\mathbf{q}_\perp) + \tilde{S}_{2C}(\mathbf{q}_\perp)|^2, \quad (30)$$

where the integration runs over the plane of perpendicular momentum transfer. The cross section (30) can be split into

the sum

$$\frac{d^3\sigma_{1C+2C}}{dk^3} = \frac{d^3\sigma_{1C}^A}{dk^3} + \frac{d^3\sigma_{2C}}{dk^3} + \frac{d^3\sigma_{\text{interf.}}}{dk^3}. \quad (31)$$

Here,

$$\frac{d^3\sigma_{1C}^A}{dk^3} = \int d^2\mathbf{q}_\perp |\tilde{S}_{1C}^A(\mathbf{q}_\perp)|^2 \quad (32)$$

and

$$\frac{d^3\sigma_{2C}}{dk^3} = \int d^2\mathbf{q}_\perp |\tilde{S}_{2C}(\mathbf{q}_\perp)|^2 \quad (33)$$

refer to the partial contributions of the single-center and two-center ionization mechanisms, respectively, whereas the term

$$\frac{d^3\sigma_{\text{interf.}}}{dk^3} = \int d^2\mathbf{q}_\perp (\tilde{S}_{1C}^A \tilde{S}_{2C}^* + (\tilde{S}_{1C}^A)^* \tilde{S}_{2C}) \quad (34)$$

arises because of interference between the direct and two-center ionization channels.

Due to the resonant nature of the two-center mechanism, one can expect that in the small vicinity $\omega_B + \epsilon_g - \Gamma^{\Delta m} \lesssim \epsilon_k \lesssim \omega_B + \epsilon_g + \Gamma^{\Delta m}$ of the resonant emission energy $\epsilon_{k_r} = \omega_B + \epsilon_g$ only the second term in (31) will be important. We have performed numerical calculations which show that, close to the resonance, the single-center and interference terms, (32) and (34), are several orders of magnitude smaller than the two-center term (33). On the other hand, in the range of emission energies far away from the resonance, the single-center channel is the dominant ionization mechanism and only the first term in (31) is important. Therefore interference between the direct and two-center channels is expected to be overall of minor importance and the interference term (34) in the cross section (31) can—to a good approximation—be neglected.

Substituting (15) into (32) and (25) into (33), we obtain

$$\frac{d^3\sigma_{1C}^A}{dk^3} = C_0 \int d^2\mathbf{q}_\perp q'^{-4} |\mathcal{F}_{\kappa_g}^{\Delta m}(\mathbf{q})|^2 \quad (35)$$

and

$$\frac{d^3\sigma_{2C}}{dk^3} = C_0 \int d^2\mathbf{q}_\perp q'^{-4} \left| \sum_{\Delta m=-1}^1 \frac{\mathcal{M}_{AB}^{\Delta m} \mathcal{F}_{eg}^{\Delta m}(\mathbf{q})}{\delta + i\Gamma^{\Delta m}/2} \right|^2, \quad (36)$$

respectively, where $C_0 = Z_P^2/(2\pi^3 v^2)$.

Since $dk^3 = \sqrt{2\epsilon_k} d\epsilon_k d\Omega_k$ the single-center and two-center ionization cross sections differential in the emission energy and solid angle read

$$\frac{d^3\sigma_{1C}^A}{d\epsilon_k d\Omega_k} = C_1 \int d^2\mathbf{q}_\perp q'^{-4} |\mathcal{F}_{\kappa_g}(\mathbf{q})|^2 \quad (37)$$

and

$$\frac{d^3\sigma_{2C}}{d\epsilon_k d\Omega_k} = C_1 \int d^2\mathbf{q}_\perp q'^{-4} \left| \sum_{\Delta m=-1}^1 \frac{\mathcal{M}_{AB}^{\Delta m} \mathcal{F}_{eg}^{\Delta m}(\mathbf{q})}{\delta + i\Gamma^{\Delta m}/2} \right|^2, \quad (38)$$

respectively, where $C_1 = Z_P^2 \sqrt{\epsilon_k}/(\sqrt{2}\pi^3 v^2)$.

Further, the energy distribution of emitted electrons is determined by the cross sections

$$\frac{d\sigma_{1C}^A}{d\epsilon_k} = \int d\Omega_k \frac{d^3\sigma_{1C}^A}{d\epsilon_k d\Omega_k} \quad (39)$$

and

$$\frac{d\sigma_{2C}}{d\varepsilon_k} = \int d\Omega_k \frac{d^3\sigma_{2C}}{d\varepsilon_k d\Omega_k} \quad (40)$$

for single-center and two-center ionization, respectively.

Finally, for the total cross sections, we obtain

$$\sigma_{1C}^A = \int_0^\infty d\varepsilon_k \frac{d\sigma_{1C}^A}{d\varepsilon_k} \quad (41)$$

and

$$\sigma_{2C} = \int_0^\infty d\varepsilon_k \frac{d\sigma_{2C}}{d\varepsilon_k}. \quad (42)$$

2. Cross section for ionization of atom B

The cross section differential in the energy and the solid angle of the electrons emitted from atom B has obviously the same form as the cross section (37) and reads

$$\frac{d^3\sigma_{1C}^B}{d\varepsilon_k d\Omega_k} = \frac{Z_P^2 \sqrt{\varepsilon_k}}{\sqrt{2\pi}^3 v^2} \int d^2\mathbf{q}_\perp q_B'^{-4} |\mathcal{F}_{\kappa_g}(\mathbf{q}_B)|^2. \quad (43)$$

Energy differential and total cross sections are obtained using expressions similar to (39) and (41).

D. Analytical cross sections for the two-center channel

Now we shall give simple approximate formulas for the two-center ionization cross sections which are expressed using single-center atomic quantities accessible from literature. Assuming that there is only one intermediate state Ψ_{ge} in atom B one can obtain that the cross section differential in the emission energy and solid angle (38) is given by

$$\frac{d^3\sigma_{2C}^{\Delta m}}{d\varepsilon_k d\Omega_k} = \frac{k}{(2\pi)^3 \delta^2 + (\Gamma^{\Delta m})^2/4} |\mathcal{M}_{AB}^{\Delta m}|^2 \sigma_{\text{exc}}^{B,\Delta m}, \quad (44)$$

where $\sigma_{\text{exc}}^{B,\Delta m}$ is the single-center cross section for excitation of atom B by ion impact and the rest on the right-hand side of this expression represents the probability that de-excitation of B results in ionization of A .

Integrating (44) over the emission angles, we obtain the cross section differential in the emission energy

$$\frac{d\sigma_{2C}^{\Delta m}}{d\varepsilon_k} = \frac{1}{2\pi} \frac{\Gamma_a^{\Delta m}}{\delta^2 + (\Gamma^{\Delta m})^2/4} \sigma_{\text{exc}}^{B,\Delta m}. \quad (45)$$

Integrating (45) over the emission energy we get the total cross section for two-center ionization

$$\sigma_{2C}^{\Delta m} = \frac{\Gamma_a^{\Delta m}}{\Gamma^{\Delta m}} \sigma_{\text{exc}}^{B,\Delta m}. \quad (46)$$

The above expression has an especially simple physical meaning: the total cross section for two-center ionization of A by ion impact is the product of the impact excitation cross section of B times the corresponding branching ratio between the two possible pathways of the de-excitation of B .

To conclude this section, we note that the quantities $|\mathcal{M}_{AB}^{\Delta m}|^2$ and $\Gamma_a^{\Delta m}$ in (44)–(46) can be very simply expressed via the radiative width Γ_r^B of the excited state of atom B and the photoionization cross section σ_{PI}^A of atom A by a photon

of frequency ω_B :

$$|\mathcal{M}_{AB}^{\Delta m}|^2 = \mathcal{A}_{\Delta m}(\mathbf{R}, \Omega_k, \omega_A) \frac{1}{k} \left(\frac{c}{\omega_B}\right)^4 \Gamma_r^B \sigma_{PI}^A(\omega_B) \quad (47)$$

and

$$\Gamma_a^{\Delta m} = \mathcal{B}_{\Delta m}(\mathbf{R}, \omega_A) \left(\frac{c}{\omega_B}\right)^4 \Gamma_r^B \sigma_{PI}^A(\omega_B). \quad (48)$$

Here, $\mathcal{A}_{\Delta m}$ and $\mathcal{B}_{\Delta m}$ are geometric factors, which depend on the internal structure of the two-center system (they are discussed in Appendix B).

III. NUMERICAL RESULTS AND DISCUSSION

A. Preliminary remarks

Here we present results of numerical calculations for ionization cross sections which are based on the theory presented in Sec. II. Throughout this section we take $Z_P = 1$. According to the first order of perturbation theory ionization cross sections depend on the projectile charge Z_P as Z_P^2 and are independent of the projectile mass. Therefore, as long as the first-order perturbative condition $Z_P/v \ll 1$ is fulfilled, the numerical results obtained for projectiles with $Z_P = 1$ can be easily generalized to collisions with bare ions with larger charges Z_P .

Besides, since in ionization by high-energy (relativistic) electrons the momentum and energy transfers to the target are negligibly small compared to the initial momentum and energy of the electron projectile (and the projectile and atomic electrons have essentially no overlap in the phase space), our results obtained for collisions with protons can be directly applied also to collisions with electrons (or positrons).

As two-center systems we shall take heteroatomic Van-der-Waals molecules Li-He [19] and Ne-He.

In Li-He, both atoms, very weakly bound by the Van-der-Waals force, are separated by quite a large mean distance $\sim 28 \text{ \AA}$ (≈ 53 a.u.) [20] while the equilibrium distance is $\sim 6.0 \text{ \AA}$ (≈ 11 a.u.) [21]. The binding energy is $\sim 0.5 \mu\text{eV}$ [20] which is much smaller than the first ionization potentials of Li ($I_A = |\varepsilon_g| = 5.39 \text{ eV}$) and He ($I_B = |\varepsilon_g| = 24.59 \text{ eV}$).

Concerning two-center ionization channel(s), here we only consider that one based on the impact excitation and consequent decay of the $1s2p$ state of He. Note that the transition $1s^2 \rightarrow 1s2p$ with an excitation energy $\omega_B = 21.22 \text{ eV}$ is the first and strongest dipole allowed transition in He. The corresponding resonance energy of the emitted electron is $\varepsilon_k = \omega_B + \varepsilon_g = 15.83 \text{ eV}$. The radiative width of the excited $1s2p$ state in He is $\Gamma_r^B = 7.44 \times 10^{-6} \text{ eV}$ [22] and the partial photoionization cross section for the $2s$ subshell in Li evaluated at ω_B is $\sigma_{PI}^A(21.22 \text{ eV}) = 7.64 \times 10^{-20} \text{ cm}^2$ [23].

In Ne-He, where the Ne and He atoms are weakly bound by the van der Waals force with the binding energy $\sim 2 \text{ meV}$ [10], the equilibrium distance is $\sim 3.0 \text{ \AA}$ (≈ 5.7 a.u.) [10] (the mean distance is close to the equilibrium one). The binding energy is four orders of magnitude smaller than the first ionization potential of Ne ($I_A = |\varepsilon_g| = 21.56 \text{ eV}$) and He ($I_B = |\varepsilon_g| = 24.59 \text{ eV}$).

For the two-center ionization of this system we consider only the channel involving the $1s^2 \rightarrow 1s3p$ transition in He

with an energy $\omega_B = 23.09$ eV. This is the first (and strongest) dipole-allowed transition in He which has an energy larger than the ionization potential of Ne (and which turned out to be extremely efficient for photoionization of a Ne-He dimer [10]). With this transition we get $\varepsilon_{k_r} = \omega_B + \varepsilon_g = 1.52$ eV for the resonant electron emission energy. The radiative width of the excited $1s3p$ state in He is $\Gamma_r^B = 2.34 \times 10^{-6}$ eV [22] and the photoionization cross section for Ne at ω_B is $\sigma_{pi}^A(23.09 \text{ eV}) = 7.05 \times 10^{-18} \text{ cm}^2$ [23].

Unlike Ne-He, the mean size of a Li-He dimer strongly differs from its equilibrium distance (≈ 53 a.u. and ≈ 11 a.u., respectively). Since the strength of the two-center ionization channel strongly depends on the interatomic distance R , the question arises on which values of R should be considered in order to provide theoretical predictions allowing for experimental verification.

In the case of a reaction, which involves fast electronic transitions resulting in a breakup of a dimer, the measurement of kinetic energies of reaction fragments quite often enables one to obtain rather accurately the magnitude of the distance R at which the process has occurred. And indeed, based on the very recent results of Ref. [24], one can expect that the most likely outcome of the two-center ionization process, which we consider, will be a break up of the Li-He dimer into Li^+ and He fragments. However, the same results (see [24]) also suggest that there is no one-to-one correspondence between the kinetic energy of the fragments and the interatomic distance R .

Therefore, in what follows, we shall only consider ionization cross sections which are averaged over the size of the vibrational ground state of the Li-He dimer. Such cross sections are obtained according to

$$\sigma_{aver} = \int_0^\infty dR \sigma(R) |\Psi_0(R)|^2, \quad (49)$$

where $\sigma(R)$ is a cross section evaluated at an interatomic distance R and $\Psi_0(R)$ is the wave function of the molecular ground state of Li-He dimer. In our calculations this state was approximated by using results of Refs. [25,26].

Since we take the interatomic interaction in the dipole-dipole form, which is valid at sufficiently large interatomic separations, the lower boundary R_{\min} of the integration over R in (49) should effectively be not 0 but instead satisfy the condition $R_{\min} \gg 1$. The latter indeed takes place due to the very rapid decrease of the probability $|\Psi_0(R)|^2$ with decreasing the interatomic distance R in the range $R \lesssim 10$ a.u. In particular, as our calculations show, depending on the type of the cross section, the difference between results obtained by setting $R_{\min} = 1$ and 10 a.u. does not exceed 1%–16%.

B. Single-center cross sections for Li, Ne, and He

For the Li-He and Ne-He systems as well for the Li, He and Ne atoms, we performed two different sets of numerical calculations. The first one is the theoretical approach presented in Secs. II A–II C.

In the second set we made use of the relativistic Bethe formula for cross sections for excitation and single ionization

of atoms. This formula reads (see, e.g., Ref. [27])

$$\sigma = \frac{8\pi Z_p^2}{v^2} \left[M^2 \left\{ \ln \left(\frac{\gamma v}{c} \right) - \frac{v^2}{2c^2} \right\} + C \right] \quad (50)$$

and is known to yield quite accurate results starting with impact energies of a few MeV/amu. Note that (50) was derived within the first order of perturbation theory in the projectile-target interaction.

The constants M^2 and C depend on the internal structure of the atomic target and can be specified for the ionization from individual subshells as well as for discrete excitations between two subshells. We extracted experimentally determined values for M^2 for the respective $2s$ and $2p$ subshell ionization of Li and Ne from [28] ($M_{\text{Li},2s}^2 = 0.515351$ and $M_{\text{Ne},2p}^2 = 1.519$). However, for these atoms we could not locate in the literature any experimental or theoretical data for the constant C . A reasonable alternative is to calculate C within the relativistic binary-encounter-Q (RBEQ) model of Ref. [29] using the above experimental values for M^2 that yields $C_{\text{Li},2s} = 3.49$ and $C_{\text{Ne},2p} = 5.89$.

In case of He, accurate theoretical values for M^2 and C exist for discrete $1s^2 \rightarrow 1snp$ ($n = 2, 3$) excitations [30] ($M_{\text{He},1s \rightarrow 2p}^2 = 0.177$, $C_{\text{He},1s \rightarrow 2p} = 0.82825$, $M_{\text{He},1s \rightarrow 3p}^2 = 0.0433$ and $C_{\text{He},1s \rightarrow 3p} = 0.20338$) as well as for ionization from the $1s^2$ ground state [31] ($M_{\text{He},1s}^2 = 0.489$ and $C_{\text{He},1s} = 2.763$).

Note also that the RBEQ model provides an analytical expression (Eq. (19) in Ref. [29]) for the energy differential ionization cross section which can be employed for calculating the single-center energy differential cross sections of Li, Ne, and He.

C. Angular distributions

In this section, we focus on the angular distribution of the emitted electrons at a resonance emission energy $\varepsilon_{k_r} = \omega_B + \varepsilon_g \equiv \varepsilon_e - \varepsilon_g + \varepsilon_g$. At this energy and in its vicinity, the ionization cross section is fully dominated by the two-center mechanism of ionization of atom A. (Moreover, as will be shown in Sec. III E, this mechanism may strongly dominate the total emission in the range of electron energies surrounding the resonance as broad as $\delta\varepsilon_k \sim 1$ eV.)

In order to explore relativistic effects in the angular distribution, in addition to relativistic calculations we performed also nonrelativistic ones in which the speed of light c was set to ∞ .

One should note that, according to both the relativistic and nonrelativistic treatments, the shape of this distribution depends on a subtle interplay between the ionization amplitudes involving ion-impact excitation of the different magnetic substates of the excited level of atom B. Since it is not possible to extract these amplitudes from cross sections, the calculation method, which was discussed in Sec. II D cannot be used here.

Figure 2 presents the angular distributions of electrons emitted with a resonance energy (≈ 15.83 eV) in the process of ionization of the Li-He system by 1 GeV protons. They are given by the cross section $\frac{d^2\sigma}{d\varepsilon_k \sin\vartheta_k d\vartheta_k}$ considered as a function of the polar emission angle ϑ_k at a given (resonance) emission energy ε_k . Two main conclusions can be drawn from this figure.

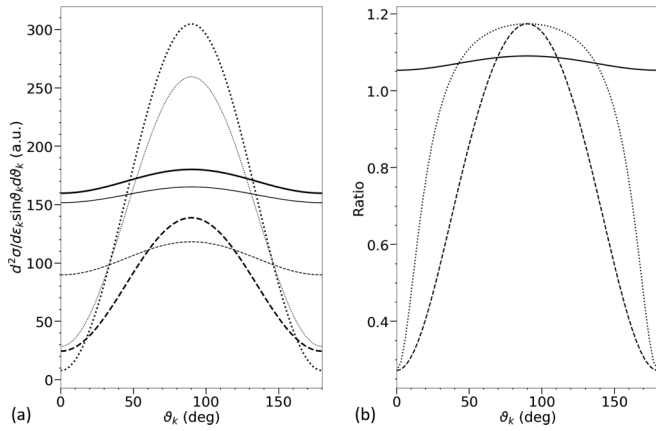


FIG. 2. (a) The angular distribution of electrons emitted with the resonance energy from the Li-He system in collisions with 1 GeV protons. The distribution was calculated by averaging over the size of the dimer and is shown for the parallel ($\mathbf{R} \parallel \mathbf{v}$, thick dashed) and perpendicular ($\mathbf{R} \perp \mathbf{v}$, thick dotted) orientation as well as for the orientational average (thick solid). In addition, the corresponding results in the nonrelativistic limit ($c \rightarrow \infty$) are displayed by thin dashed, thin dotted and thin solid curves, respectively. (b) The relativistic-to-nonrelativistic cross section ratio for $\mathbf{R} \parallel \mathbf{v}$ (dashed), $\mathbf{R} \perp \mathbf{v}$ (dotted) and the orientational average (solid).

First, all the angular distributions are symmetric with respect to the emission angle $\vartheta_k = 90^\circ$. This feature arises because the two-center ionization is driven solely by dipole transitions (including those leading to the excitation of atom B and those resulting in the consequent energy exchange between B and A). Note that this feature is absent in the direct ionization of A (or B) where the interference between the dipole and nondipole (mainly quadrupole) transitions leads to an asymmetry between the angular ranges $\vartheta_k \leq 90^\circ$ and $\vartheta_k \geq 90^\circ$ (with more electrons being emitted into the forward semisphere $\vartheta_k \leq 90^\circ$).

Second, at an impact energy of 1 GeV/amu (which corresponds to a rather modest value of the collisional Lorentz factor of $\gamma \approx 2.1$), the shape of the angular distribution of the emitted electrons is already very substantially influenced by relativistic effects which enhance the emission into the transverse direction and decrease it parallel/antiparallel to the collision velocity. As additional calculations show, such a redistributive action of the relativistic effects remains for any orientation of the dimer (even though its strength depends on the orientation). This feature can be understood by noting that in high-energy ion-atom collisions, in which the motion of atomic electrons remains nonrelativistic, the main relativistic effect is caused by the flattening of the electric field generated by the projectile. This flattening increases the electric field in the transverse ($\perp \mathbf{v}$) direction and reduces its component parallel/antiparallel to the projectile velocity which leads to the enhancement of the emission in the transverse direction and its reduction in the longitudinal direction(s).

Third, after averaging over the orientation of the dimer the angular distribution of electrons emitted via the two-center ionization channel turns out to be rather weakly dependent on the polar emission angle: it is almost spherically symmetric. This means that, in case of two-center ionization, the angu-

lar momentum, which is imparted into the initial system in the collision (due to the absorption of a virtual photon), on average mainly goes to the nuclei leading to excitation of rotational degrees of freedom of the residual $(\text{Li-He})^+$ system.

The very pronounced maximum in the electron emission at $\vartheta_k = 90^\circ$, which is present both at $\mathbf{R} \parallel \mathbf{v}$ and $\mathbf{R} \perp \mathbf{v}$, and the rather weak dependence of the electron emission on ϑ_k , when the averaging over the orientation of the dimer is performed, show that the shape of the emission pattern has a nontrivial dependence on the angle $\theta_R = \arccos(\mathbf{R} \cdot \mathbf{v}/Rv)$. In particular, our numerical calculations show that provided $0^\circ \leq \theta_R \lesssim 18^\circ$ or $63^\circ \lesssim \theta_R \leq 90^\circ$ the angular distribution of the emitted electrons has a maximum at $\vartheta_k = 90^\circ$ and two equal minima at $\vartheta_k = 0^\circ$ and $\vartheta_k = 180^\circ$, whereas if $18^\circ \lesssim \theta_R \lesssim 63^\circ$ then the electron emission has two equal maxima at $\vartheta_k = 0^\circ$ and $\vartheta_k = 180^\circ$ and a minimum at $\vartheta_k = 90^\circ$.

An analytical evaluation of the two-center cross sections could give a better idea about the orientation dependence of the emission. By using the theoretical approach of our paper this is quite cumbersome, though. However, within the Weizsäcker-Williams approximation, in which the field of a relativistic charged projectile is replaced by “equivalent photons” (which is rather accurate at high impact energies), one can show that the angular distribution of the electrons emitted via the two-center channel is given by

$$\frac{d^2\sigma}{d\varepsilon_k \sin \vartheta_k d\vartheta_k} \sim A(\theta_R) \sin^2 \vartheta_k + B(\theta_R) \cos^2 \vartheta_k, \quad (51)$$

where

$$A(\theta_R) = \frac{1 + (3 \sin^2 \theta_R - 1)^2}{2},$$

$$B(\theta_R) = 9 \sin^2 \theta_R \cos^2 \theta_R. \quad (52)$$

While being simple, expression (51) captures all essential features of the results of our numerical calculations (based on a formalism which is more general and more accurate than the Weizsäcker-Williams approximation). In particular, (i) it shows that when the dimer is parallel or perpendicular to the collision velocity the angular distribution is proportional to $\sin^2 \vartheta_k$ and also predicts that at the dimer orientation $\theta_R = 90^\circ$, the emission is 2.5 times larger than at $\theta_R = 0^\circ, 180^\circ$ (note that from our numerical calculations, we obtain for this ratio ≈ 2.2).

(ii) Expression (51) also predicts that when the angle θ_R varies between $17^\circ \lesssim \theta_R \lesssim 58^\circ$ one has $B(\theta_R) > A(\theta_R)$ implying that in this interval of θ_R the electron emission has maxima at $\vartheta_k = 0^\circ, 180^\circ$, and a minimum at $\vartheta_k = 90^\circ$ (note that the above interval is quite close to the interval $18^\circ \lesssim \theta_R \lesssim 63^\circ$ following from our numerical calculations).

(iii) After averaging expression (51) over the dimer orientation, we obtain for the angular emission distribution

$$\left\langle \frac{d^2\sigma}{d\varepsilon_k \sin \vartheta_k d\vartheta_k} \right\rangle \sim \left(1 + \frac{1}{6} \sin^2 \vartheta_k \right), \quad (53)$$

which predicts a modest maximum in the electron emission at $\vartheta_k = 90^\circ$. According to (53) the emission at 90° exceeds that at 0° and 180° by about 16%–17% which is somewhat larger compared to our full numerical calculations where we get about 10%–15%.

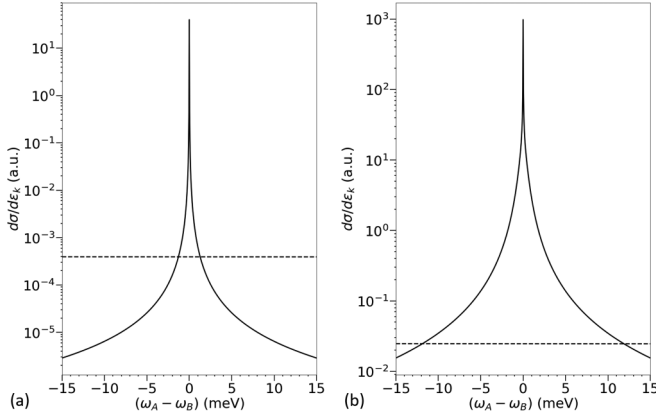


FIG. 3. (a) The energy distribution of emitted electrons as a function of the detuning $\delta = \omega_A - \omega_B$ for the Li-He system for two-center ionization (solid) and direct ionization of Li (dashed) in collisions with 1 GeV protons. The two-center distribution was calculated by averaging over the internuclear vector \mathbf{R} of the dimer. (b) The corresponding energy distribution for the Ne-He system for two-center ionization (solid) and direct ionization of Ne (dashed). The two-center distribution was obtained by averaging over the orientation of the dimer at a fixed interatomic distance $R = 3 \text{ \AA}$.

The shape of the orientation-averaged angular distribution for Li-He qualitatively differs not only from those at $\mathbf{R} \parallel \mathbf{v}$ and $\mathbf{R} \perp \mathbf{v}$ but also from that for ionization from an s state of a single atom which is characterized by a pronounced emission maximum at $\vartheta_k \approx 90^\circ$ and very little emission in the forward, $\vartheta_k \approx 0^\circ$, and backward, $\vartheta_k \approx 180^\circ$, directions. Since the range of emission energies $\delta\epsilon_k \sim 1 \text{ eV}$ surrounding the resonance is strongly dominated by the two-center channel (see Sec. III E), the overall angular distribution of the emitted electrons in this range will qualitatively differ from that typical for single Li and He atoms (and also for a Li-He dimer very far from the resonance).

Effects similar to those, which were discussed for Li-He, arise also in the impact ionization of Ne-He dimers. In particular, relativistic effects tend to increase electron emission in the transverse direction and decrease it in the longitudinal directions. Besides, after averaging over the dimer orientation the shape of the emission spectrum substantially differs from those arising in the impact ionization of single Ne and He atoms.

D. Energy distributions

In this section, we consider the energy distribution of electrons emitted from the two-center systems represented by Li-He and Ne-He dimers. In Fig. 3, we display the energy distribution of emitted electrons in the process of ionization of Li-He and Ne-He by 1 GeV protons. It is determined by the cross section $\frac{d\sigma}{d\epsilon_k}$ taken as a function of the energy detuning $\delta = \omega_A - \omega_B$. In this figure, we show the two-center cross section, which is given by the (incoherent) sum of partial cross sections (45) over all intermediate states Ψ_{ge} of the two-center system, and the single-center cross sections for the ionization of Li and Ne (the latter were obtained using Eq. (19) of Ref. [29]).

As can be seen in Fig. 3, the two-center cross section has a resonant structure, reaching a maximum at the respective resonance energy $\epsilon_{k_r} = \omega_B + \epsilon_g$, and rapidly decreases for both $\epsilon_k < \epsilon_{k_r}$ and $\epsilon_k > \epsilon_{k_r}$. The width of the resonance is determined by the total decay width Γ which consists of the radiative width (23) and two-center autoionization width (24). The single-center cross sections depend only slightly on the electron emission energy ϵ_k .

In a narrow vicinity of the resonance emission energy, two-center ionization can dominate direct ionization by several orders of magnitude. In particular, the ratio of two-center and single-center cross section

$$\mu^{(1)} = \frac{d\sigma_{2C}/d\epsilon_k}{d\sigma_{1C}^A/d\epsilon_k} \quad (54)$$

evaluated at the resonance becomes $\approx 10^5$ for Li-He and $\approx 4 \times 10^4$ for Ne-He, respectively. Outside the resonant energy interval, $\omega_B + \epsilon_g - \Gamma \lesssim \epsilon_k \lesssim \omega_B + \epsilon_g + \Gamma$, two-center ionization strongly diminishes and the direct ionization channel dominates.

We mention that the two-center cross section in the relativistic treatment is $\sim 7.5\%$ larger than its corresponding nonrelativistic limit ($c \rightarrow \infty$) for both the Li-He and Ne-He system.

In our consideration, the dimer is regarded as a system of two independent atoms which interact with each other but otherwise keep their identities. In reality, even a very weakly bound dimer is a molecule and its interaction with the projectile ion will in general involve excitation not only of electronic but also of vibrational and rotational states of the dimer. As a result, the spectrum of the emitted electrons will be split into several lines corresponding to the involvement of different vibrational (and rotational) states into the process [10,11,26]. However, since these states have much smaller energy separations than electronic states, the electron emission lines will be quite close to each other. Therefore the electron spectrum, after averaging over the energy interval containing all the lines, is expected to correspond to that one predicted by our two-atomic model of this process (provided this electron spectrum is also averaged over the same energy interval). The same can also be said about the enhancement in ionization, which is due to the presence of the two-center channel.

E. Total cross section

In this section, we consider the total cross section for electron emission from the two-center system as a function of the projectile energy. Figure 4 shows the dependence of the total two-center ionization cross section, given by the sum of partial cross sections (46), on the projectile energy (per nucleon) E_p for the Ne-He system together with the single-center cross sections for single ionization of Ne and He atoms.

We can conclude from Fig. 4 that the two-center and single-center cross sections for the ionization of atom A show the same asymptotic behavior for high projectile energies. This results from two facts: first, the dependence of σ_{2C} in (46) on the impact energy is solely determined by the energy dependence of the impact excitation cross section σ_{exc}^B ; second, at high impact energies the cross sections for ionization

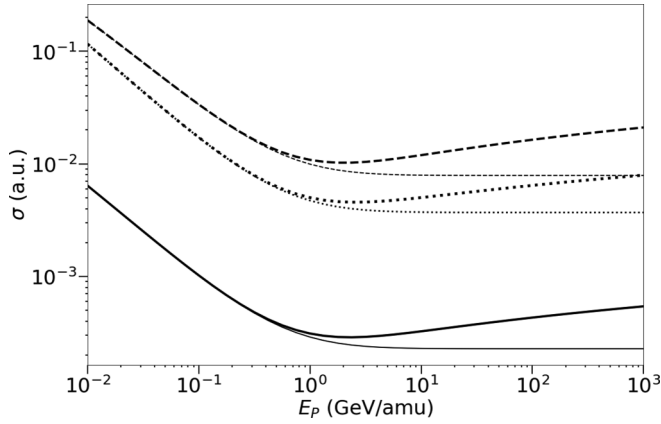


FIG. 4. Total cross section, given as a function of the projectile energy (per nucleon) E_p , for two-center ionization of Ne-He (thick solid) and direct ionization of Ne (thick dashed) and He (thick dotted) atoms. The two-center cross section was calculated by averaging over the orientation of the dimer for a fixed interatomic distance $R = 3 \text{ \AA}$. In addition, we show the corresponding cross sections obtained neglecting the relativistic effects ($c \rightarrow \infty$, by thin solid, thin dashed and thin dotted curves, respectively).

and dipole-allowed excitations show quite a similar dependence on E_p .

In order to characterize the overall effect of the two-center channel on the total emission from A , we evaluated the ratio

$$\mu^{(2)} = \frac{\sigma_{2C}}{\sigma_{1C}^A} \quad (55)$$

of total two-center and single-center cross sections at $E_p = 1 \text{ GeV/amu}$ obtaining 3.8×10^{-4} and 2.9×10^{-2} for Li-He and Ne-He, respectively. Thus, for Li-He, the two-center channel adds very little to the total emission from Li while for Ne-He, which has much smaller size, the two-center ionization mechanism gives a more noticeable contribution to the total emission from Ne.

The relative overall weakness of the two-center channel in ionization of Li-He is caused by two main reasons. First, the size of this dimer is much larger than that of Ne-He which weakens the atom-atom interaction. Second, the frequency ω_B of the $1s^2 \rightarrow 1s2p$ transition in He is about 21 eV that results in the emission of electrons from Li with kinetic energy of about 16 eV, which is by a factor of 3 larger than the ionization potential of Li, whereas in case of Ne-He the two-center resonance due to the $1s^2 \rightarrow 1s3p$ transition in He with the frequency $\omega_B \approx 23 \text{ eV}$ results in emission of electrons with energies about 2 eV, which is much smaller than the ionization potential of Ne. Since it is known that in fast collisions with charged projectiles most of the emitted electrons have energies not exceeding their initial atomic binding energy, it is not very surprising that the range of relatively large emission energies ($\sim 16 \text{ eV}$) contributes much less the emission from Li than the range of low emission energies ($\sim 2 \text{ eV}$) to the ionization of Ne.

Even though the two-center channel turns out to contribute little to the total emission one should note the following. If we limit the integration to an interval of emission energies centered at the resonance and having the width $\delta\epsilon_k \approx 0.5 \text{ eV}$,

which is much smaller than the “effective width” of the atomic continuum ($\sim 10 \text{ eV}$) but several orders of magnitude larger than the resonance width, the ratio (55) becomes $\mu^{(2)} \approx 174$ for Li-He and $\mu^{(2)} \approx 200$ for Ne-He. Hence, in a not very large ($\delta\epsilon_k \sim 1 \text{ eV}$) but experimentally very well resolved range of emission energies containing the resonance, the two-center ionization channel still very strongly outperforms the direct ionization channel.

Up to now we only have discussed electron emission from atom A (via the direct and two-center channels) but have not yet considered single-center ionization of atom B which also contributes to electron emission from the whole A - B system. The direct impact ionization of B leads to an enhancement of the background of ejected electrons as well as a decrease in the total number of neutral atomic species B which are essential for two-center ionization to take place. The latter point remains of minor importance (as long as the condition $Z_p/v \ll 1$ is fulfilled). However, the direct ionization of B may substantially contribute to the total emission (that, in particular, reduces the role of the two-center ionization) and should be taken into account.

The influence of the two-center channel on the total emission from both atomic centers may be characterized by the ratio

$$\mu^{(3)} = \frac{\sigma_{2C}}{\sigma_{1C}^A + \sigma_{1C}^B} \quad (56)$$

of total two-center and “ $A + B$ ” single-center cross sections. Considering only the interval of emission energies centered at the resonance and having the width $\delta\epsilon_k \approx 0.5 \text{ eV}$, we obtain $\mu^{(3)} \approx 8.3$ for Li-He and $\mu^{(3)} \approx 152$ for Ne-He. This could be compared with the ratio (55) for the same energy interval which gives ≈ 174 for Li-He and ≈ 200 for Ne-He as already mentioned. Hence, inclusion of electron emission from He strongly reduces the relative contribution of two-center ionization in the Li-He dimer while the corresponding effect for the Ne-He dimer is rather weak. Nevertheless, the two-center channel remains highly visible even in the case of Li-He dimers.

The cross section of the total (single) ionization of He atoms is shown in Fig. 4. Over the displayed range of impact energies, the electron emission from a Li atom is between 15% and 37% larger than that from He whereas the direct emission from Ne atom turns out to be substantially larger than from He dominating the latter by a factor of 1.62 to 2.65. Thus, for the Li-He system, the direct ionization of He can not be neglected while for Ne-He, it is not very important.

The two-center and single-center cross sections in the relativistic treatment which are displayed in Fig. 4 show a logarithmic growth starting with projectile energies of a few GeV/amu. This is a typical relativistic effect observed for all dipole-allowed transitions which is caused by the flattening of the electromagnetic field of the projectile. In the nonrelativistic limit ($c \rightarrow \infty$), the flattening disappears, the logarithmic growth is naturally absent and all the calculated cross sections simply “saturate.”

E. Retardation effects in two-center ionization

Let us now briefly consider the role of retardation effects in the two-center system which are caused by the finite

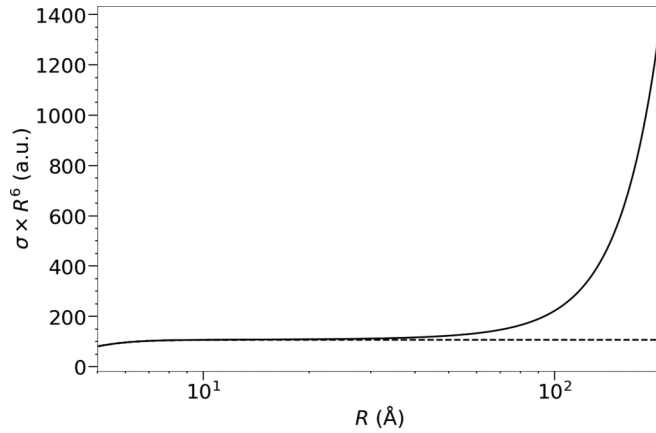


FIG. 5. Total cross section at $E_p = 1$ GeV/amu for Li-He dimer multiplied by R^6 as a function of the interatomic distance R using the retarded dipole-dipole interaction (3) (solid) and the instantaneous interaction (4) (dashed). The cross section was averaged over the orientation of the dimer.

propagation time of the electromagnetic field transmitting the interaction between the two atoms. Figure 5 displays the total two-center cross section, given by the sum of partial cross sections (46), for Li-He multiplied by R^6 as a function of the interatomic distance R between A and B . The cross section was evaluated using either the retarded dipole-dipole interaction (3) or its instantaneous limit given by (4).

In general, the importance of the retardation effects depends on the ratio between the electronic transition time $\tau = \frac{1}{\omega_B}$ and the time $T = \frac{R}{c}$ necessary for the electromagnetic field to propagate between the atoms: if $T \ll \tau$ then the field propagates essentially instantaneously whereas at $T \gg \tau$ the retardation effects very strongly influence the two-center interaction [in the latter case Eqs. (3) and (4) predict the $1/R$ and $1/R^3$ dependencies, respectively].

Since the size of the He-Ne dimer is relatively small (and the transition time does not exceed 1 a.u.), for the two-center ionization of this dimer the retardation effects are expected to be negligible (this also follows from our calculations for the cross section).

In contrast, for the Li-He dimer the transition time τ is also close to 1 a.u. but the mean size is much larger reaching about 53 a.u.. In this case the ratio $\eta = T/\tau = \frac{\omega_B R}{c}$ is not very small ($\eta \approx 0.3$) and one could expect a sizable retardation effect.

However, according to the calculation (see Fig. 5) the retardation effects in fact become of importance only at distances which are noticeably larger than the above simple estimates suggest. In particular, in the case of two-center ionization of Li-He, the effect of the retardation in the atom-atom interaction on the ionization (averaged over the dimer size) turned out to be below 1%.

Instead of focusing on very large dimers with relatively low transition frequencies, one could consider ionization of a relatively small dimer but involving much higher values of the transition frequency. Suppose that the active electron in atom B undergoes a dipole-allowed transition between states where it is effectively restricted to the space region around the nucleus with a linear size a_B . Then its dipole matrix elements will be $\sim a_B$ whereas its transition frequencies ω_B

would scale as $\omega_B \sim a_B^{-2}$. Let $a_B \simeq 0.1$ a.u. and, consequently, $\omega_B \simeq 10^2$ a.u. In such a case, retardation effects in the interaction of an atom B with its neighbor atom A would become of importance beginning already with the interatomic distances $R \simeq 1$ a.u. This simple consideration suggests that the influence of retardation effects on the two-center ionization channel would become substantial if the active electron in atom B is (initially) tightly bound. However, as estimates show, the retardation effects become important only when the two-center channel itself is already rather weak.

IV. SUMMARY

We have considered single-electron emission from a heteroatomic system, consisting of two weakly bound atomic species A and B , in relativistic collisions with charged projectiles. Provided that the ionization potential of A is smaller than an excitation energy for a dipole-allowed transition in B , three single ionization channels occur: (i) single-center ionization of atom A , (ii) single-center ionization of atom B , and (iii) two-center ionization of A . Channels (i) and (ii) describe the well known mechanism of direct impact ionization of a single atom while in channel (iii) ionization of A involves the impact excitation of B with subsequent radiationless transfer of the excitation energy—via (long-range) interatomic electron correlations—to A , resulting in its ionization.

Our theoretical approach to collisions between the A - B system and the projectile was based on the semiclassical approximation which is very well justified at high impact velocities and in which the relative motion of the nuclei is treated classically while the active electrons are considered quantum mechanically. The above three reaction channels were described using the lowest (possible) order of perturbation theory. Namely, the single-center channels were treated using the first order of perturbation theory in the projectile-atom interaction whereas the amplitude for the two-center channel was obtained within the second order of perturbation theory, where both the interaction of the projectile with atom B and the interatomic interaction between A and B are present.

We have applied our approach to study ionization of the Li-He and Ne-He dimers. Since the mean size of and the equilibrium interatomic distance in Ne-He are close (both are ≈ 3 Å), the calculations for this system were performed at a fixed value $R = 3$ Å. In case of Li-He, where the mean size and the equilibrium distance strongly differ, the calculations were done by averaging results for a fixed R over the vibrational ground state of Li-He. A few main conclusions can be drawn from our study.

First, substantial relativistic effects in ionization of a weakly bound dimer are caused by the flattening of the electric field of the projectile in the transverse direction which arises when the collision velocity becomes comparable to the speed of light. However, the role of the other type of relativistic effects—the retardation in the interaction between the atoms of the dimer—turned out to be weaker than one could expect being very small even for the Li-He dimer whose mean size (28 Å ≈ 53 a.u.) is very large on the atomic scale.

Second, the relativistic effects in ionization become visible first of all in the angular distributions of emitted electrons where they reach substantial magnitude already at modest

relativistic impact energies corresponding to $\gamma \sim 1-2$. These effects increase the emission into the transverse direction and decrease it in the longitudinal direction (counted from the collision velocity).

Third, the influence of the relativistic effects on the energy spectra of emitted electrons and the total ionization cross section noticeably increases the latter but a substantial increase can be reached only at quite high impact energies (corresponding to $\gamma \gg 1$).

Fourth, in the close vicinity of the resonance energy the two-center channel becomes so strong that its contribution continues to dominate ionization for the whole range of emission energies ($\delta\varepsilon_k \sim 1$ eV) which contains the resonance but is orders of magnitude broader than the width of the resonance. This coincides with our previous finding for ionization by nonrelativistic electrons [15].

Our theoretical predictions can be tested in experiments where Li-He and/or Ne-He dimers are bombarded by high-energy charged particles. We note, in particular, that the Ne-He dimer was already used in recent experiments on the related process of two-center resonant photoionization [10,11].

ACKNOWLEDGMENT

We acknowledge the support from the Deutsche Forschungsgemeinschaft (DFG, German Research Foundation) under Grant No 349581371 (MU 3149/4-1 and VO 1278/4-1).

APPENDIX A

Here we shall derive the dipole-dipole interaction \hat{V}_{AB} between atoms A and B given by equation (3). There are different ways to obtain this interaction, including those where the electromagnetic field is considered as quantized, see, e.g., Ref. [32], but here we will derive it using an approach, in which the electromagnetic field is regarded as classical (and which we could not locate in the literature). Considering the coupling $j_\mu^A A_B^\mu$ between the transition four-current $j_\mu^A = (c\rho_A, \mathbf{j}_A)$ of the electron in atom A and the four-potential $A_B^\mu = (\phi, \mathbf{A})$ of the field created by the other electron in atom B , the corresponding first-order transition amplitude is given by

$$a_{fi}^{(1)} = -\frac{i}{c^2} \int d^4x j_\mu^A(x) A_B^\mu(x) \quad (\text{A1})$$

with $x^\mu = (ct, \mathbf{x})$ the four-space-time vector. The four-potential $A_B^\mu(x)$ satisfies the Maxwell equations

$$\square A_B^\mu(x) = -\frac{4\pi}{c} j_B^\mu(x). \quad (\text{A2})$$

First, we apply the inverse Fourier transforms

$$\begin{aligned} j_\mu^A(x) &= \frac{1}{(2\pi)^2} \int d^4k_A \tilde{j}_\mu^A(k_A) e^{-ik_A x}, \\ A_B^\mu(x) &= \frac{1}{(2\pi)^2} \int d^4k_B \tilde{A}_B^\mu(k_B) e^{-ik_B x}, \end{aligned} \quad (\text{A3})$$

where $k_A^\mu = (\omega'_A/c, \mathbf{k}_A)$ and $k_B^\mu = (\omega'_B/c, \mathbf{k}_B)$ are the four-wave vectors of the electrons in A and B . Insertion of (A3)

into (A1) and subsequent integration over space-time yields

$$a_{fi}^{(1)} = -\frac{i}{c^2} \int d^4k_A \tilde{j}_\mu^A(k_A) \tilde{A}_B^\mu(-k_A). \quad (\text{A4})$$

Further, we can solve (A2) in the four-dimensional k_B space and get

$$\tilde{A}_B^\mu(k_B) = \frac{4\pi}{c} \tilde{G}_F(k_B) \tilde{j}_B^\mu(k_B). \quad (\text{A5})$$

Here, $\tilde{G}_F(k_B) = ((\omega'_B/c)^2 - \mathbf{k}_B^2 + i\eta)^{-1}$ ($\eta > 0$) is the Feynman propagator for a massless Klein-Gordon particle. If we take into account (A5), the transition amplitude in (A4) becomes

$$a_{fi}^{(1)} = -\frac{4\pi i}{c^3} \int d^4k_A \tilde{G}_F(-k_A) \tilde{j}_\mu^A(k_A) \tilde{j}_B^\mu(-k_A). \quad (\text{A6})$$

Using the Fourier transform, the four-currents in (A6) can be written as

$$\begin{aligned} \tilde{j}_\mu^A(k_A) &= \frac{1}{(2\pi)^2} \int d^4x j_\mu^A(x) e^{ik_A x}, \\ \tilde{j}_B^\mu(-k_A) &= \frac{1}{(2\pi)^2} \int d^4x j_B^\mu(x) e^{i(-k_A)x}. \end{aligned} \quad (\text{A7})$$

Now, taking into account that the motion of the electrons is nonrelativistic, we approximate $j_\mu^A(x)$ and $j_B^\mu(x)$ in (A7) by the Schrödinger transition four-currents which read (see, e.g., Ref. [33]):

$$\begin{aligned} j_\mu^A(x) &= (c\phi_f^*(\mathbf{r})\phi_i(\mathbf{r})e^{i\omega_A t}, \\ &\quad -\frac{1}{2}\{\phi_f^*(\mathbf{r})\hat{\mathbf{p}}_x\phi_i(\mathbf{r}) + \phi_i(\mathbf{r})\hat{\mathbf{p}}_x\phi_f^*(\mathbf{r})\}e^{i\omega_A t}), \\ j_B^\mu(x) &= (c\chi_f^*(\boldsymbol{\xi})\chi_i(\boldsymbol{\xi})e^{i\omega_B t}, \\ &\quad \frac{1}{2}\{\chi_f^*(\boldsymbol{\xi})\hat{\mathbf{p}}_x\chi_i(\boldsymbol{\xi}) + \chi_i(\boldsymbol{\xi})\hat{\mathbf{p}}_x\chi_f^*(\boldsymbol{\xi})\}e^{i\omega_B t}), \end{aligned} \quad (\text{A8})$$

where ϕ_i (χ_i) is the initial state of atom A (B), ϕ_f (χ_f) the final state of A (B) and $\hat{\mathbf{p}}_x = \frac{1}{i}\nabla_x$ the momentum operator. Inserting (A8) into (A7), calculating the resulting time integrals and inserting these results into (A6), we obtain

$$\begin{aligned} a_{fi}^{(1)} &= -\frac{i}{4\pi c^2} \int_{-\infty}^{\infty} d\omega'_A \delta(\omega_A + \omega'_A) \delta(\omega_B - \omega'_A) \\ &\quad \times \langle \phi_f \chi_f | (2c)^2 \mathcal{I} - \mathcal{I} \hat{\mathbf{p}}_r \hat{\mathbf{p}}_\xi - \hat{\mathbf{p}}_\xi \mathcal{I} \hat{\mathbf{p}}_r \\ &\quad - \hat{\mathbf{p}}_r \mathcal{I} \hat{\mathbf{p}}_\xi - \hat{\mathbf{p}}_r \hat{\mathbf{p}}_\xi \mathcal{I} | \phi_i \chi_i \rangle, \end{aligned} \quad (\text{A9})$$

where

$$\mathcal{I} = \int d^3\mathbf{k}_A \tilde{G}_F(-k_A) e^{-i\rho \cdot \mathbf{k}_A} \quad (\text{A10})$$

with $\rho = \mathbf{R} + \mathbf{r} - \boldsymbol{\xi}$. Integration over the solid angle $\Omega_{\mathbf{k}_A}$ in (A10) provides

$$\mathcal{I} = \frac{2\pi i}{\rho} \int_{-\infty}^{\infty} dk_A \frac{k_A e^{-i\rho k_A}}{(\omega'_A/c)^2 - k_A^2 + i\eta}. \quad (\text{A11})$$

The remaining integral in (A11) is solved by applying the residual theorem and we arrive at

$$\mathcal{I} = 2\pi^2 \frac{e^{i\rho \frac{|\omega'_A|}{c}}}{\rho}. \quad (\text{A12})$$

Inserting (A12) into (A9), afterwards calculating the ω'_A integral by taking advantage of one of the delta functions and recalling that $\omega_A = \varepsilon_k - \varepsilon_g > 0$ yields

$$a_{fi}^{(1)} = \frac{2\pi}{i} \delta(\omega_A + \omega_B) \langle \phi_f \chi_f | \frac{1}{(2c)^2} \left\{ (2c)^2 \frac{e^{i\rho \frac{\omega_A}{c}}}{\rho} - \frac{e^{i\rho \frac{\omega_A}{c}}}{\rho} \hat{\mathbf{p}}_r \hat{\mathbf{p}}_\xi - \hat{\mathbf{p}}_\xi \frac{e^{i\rho \frac{\omega_A}{c}}}{\rho} \hat{\mathbf{p}}_r - \hat{\mathbf{p}}_r \frac{e^{i\rho \frac{\omega_A}{c}}}{\rho} \hat{\mathbf{p}}_\xi - \hat{\mathbf{p}}_r \hat{\mathbf{p}}_\xi \frac{e^{i\rho \frac{\omega_A}{c}}}{\rho} \right\} | \phi_i \chi_i \rangle. \quad (\text{A13})$$

Considering the interaction \hat{V}_{AB} between the two electrons in atom A and B as a small perturbation, the quantum mechanical transition amplitude within the first order of perturbation theory reads

$$a_{fi}^{(1)} = \frac{2\pi}{i} \delta(\omega_A + \omega_B) \langle \phi_f \chi_f | \hat{V}_{AB} | \phi_i \chi_i \rangle. \quad (\text{A14})$$

Comparing (A13) and (A14), the interaction \hat{V}_{AB} is given by

$$\hat{V}_{AB} = \frac{1}{(2c)^2} \left\{ (2c)^2 \frac{e^{i\rho \frac{\omega_A}{c}}}{\rho} - \frac{e^{i\rho \frac{\omega_A}{c}}}{\rho} \hat{\mathbf{p}}_r \hat{\mathbf{p}}_\xi - \hat{\mathbf{p}}_\xi \frac{e^{i\rho \frac{\omega_A}{c}}}{\rho} \hat{\mathbf{p}}_r - \hat{\mathbf{p}}_r \frac{e^{i\rho \frac{\omega_A}{c}}}{\rho} \hat{\mathbf{p}}_\xi - \hat{\mathbf{p}}_r \hat{\mathbf{p}}_\xi \frac{e^{i\rho \frac{\omega_A}{c}}}{\rho} \right\}. \quad (\text{A15})$$

The interaction in (A15) includes all kinds of multipole-interactions between the two electrons in A and B . Since we are only interested in the strongest coupling, namely the dipole-dipole interaction, between the electrons, we employ appropriate multipole expansions in the term $e^{i\rho \frac{\omega_A}{c}} / \rho$ in (A15). First, we expand $1/\rho$ up to second order in $\mathbf{h} = \mathbf{r} - \boldsymbol{\xi}$. Afterwards, an expansion of ρ in the exponent, again up to second order in \mathbf{h} , is made. Finally, we expand the resulting exponential terms up to second order in \mathbf{h} . Keeping only terms up to second order in \mathbf{h} in the final result, we get

$$\frac{e^{i\rho \frac{\omega_A}{c}}}{\rho} \approx \left\{ \frac{1}{R} - \frac{[(\mathbf{r} - \boldsymbol{\xi}) \cdot \mathbf{R}]^2}{2R^3} \left(\frac{\omega_A}{c} \right)^2 + \left(\frac{3[(\mathbf{r} - \boldsymbol{\xi}) \cdot \mathbf{R}]^2}{2R^5} - \frac{(\mathbf{r} - \boldsymbol{\xi})^2}{2R^3} - \frac{(\mathbf{r} - \boldsymbol{\xi}) \cdot \mathbf{R}}{R^3} \right) \times \left(1 - iR \frac{\omega_A}{c} \right) \right\} e^{iR \frac{\omega_A}{c}}. \quad (\text{A16})$$

Now, we insert (A16) into (A15) and use the identities $\hat{\mathbf{p}}_r = i\omega_A \mathbf{r}$ and $\hat{\mathbf{p}}_\xi = i\omega_B \boldsymbol{\xi} = i(-\omega_A) \boldsymbol{\xi}$ which arise from the commutator relations $\hat{\mathbf{p}}_r = i[\hat{H}_A, \mathbf{r}]$ and $\hat{\mathbf{p}}_\xi = i[\hat{H}_B, \boldsymbol{\xi}]$. Afterwards, we neglect all terms in the resulting interaction \hat{V}_{AB} that will not lead to dipole allowed transitions. Our final result for the dipole-dipole interaction \hat{V}_{AB} then becomes

$$\hat{V}_{AB} = e^{iR \frac{\omega_A}{c}} \left[\left(\mathbf{r} \cdot \boldsymbol{\xi} - \frac{3(\mathbf{r} \cdot \mathbf{R})(\boldsymbol{\xi} \cdot \mathbf{R})}{R^2} \right) \frac{1 - iR \frac{\omega_A}{c}}{R^3} - \left(\mathbf{r} \cdot \boldsymbol{\xi} - \frac{(\mathbf{r} \cdot \mathbf{R})(\boldsymbol{\xi} \cdot \mathbf{R})}{R^2} \right) \frac{\left(\frac{\omega_A}{c} \right)^2}{R} \right]. \quad (\text{A17})$$

APPENDIX B

In order to evaluate the two-center ionization cross sections defined in Sec. II D. for the systems Li-He and Ne-He, we have calculated the corresponding geometric factors $\mathcal{A}_{\Delta m}$ and $\mathcal{B}_{\Delta m}$ in (47) and (48).

More precisely, for fixed principal quantum numbers n_A and n'_A and n_B and n'_B in atoms A and B , respectively, in case of Li-He, $\mathcal{A}_{\Delta m}$ and $\mathcal{B}_{\Delta m}$ were derived for all possible $n_{BS} \rightarrow n'_B p_m$ ($m \in \{-1, 0, 1\}$) bound-bound transitions (3 in total) in B for a fixed $n_{AS} \rightarrow \varepsilon_k p$ bound-continuum transition in A . Further, in case of Ne-He, $\mathcal{A}_{\Delta m}$ and $\mathcal{B}_{\Delta m}$ were derived for all combinations (9 in total) of $n_{APm_A} \rightarrow \varepsilon_k d$ ($m_A \in \{-1, 0, 1\}$) bound-continuum transitions in A and $n_{BS} \rightarrow n'_B p_m$ bound-bound transitions in B . Here, one should mention that the dipole selection rules would also allow $n_{AP} \rightarrow \varepsilon_k s$ transitions in A , but for rare gases in general [34] and especially for the $2p$ subshell in Ne [35,36] the main contribution to the n_{AP} -subshell ionization cross section comes from $n_{AP} \rightarrow \varepsilon_k d$ transitions, so we only consider these.

(i) Geometric factors $\mathcal{A}_{\Delta m}(\mathbf{R}, \Omega_k, \omega_A)$ and $\mathcal{B}_{\Delta m}(\mathbf{R}, \omega_A)$ for the $n_{AS} \rightarrow \varepsilon_k p$ bound-continuum transition in atom A and $n_{BS} \rightarrow n'_B p_m$ ($m \in \{-1, 0, 1\}$) bound-bound transitions in atom B :

$$\begin{aligned} \mathcal{A}_0 &= \frac{9}{16} |\mathbf{e}_k \cdot \boldsymbol{\rho}_0|^2, & \mathcal{A}_{\pm 1} &= \frac{9}{32} |\mathbf{e}_k \cdot \boldsymbol{\rho}_{\pm 1}|^2, \\ \mathcal{B}_0 &= \frac{3}{16\pi} [|(\boldsymbol{\rho}_0)_x|^2 + |(\boldsymbol{\rho}_0)_y|^2 + |(\boldsymbol{\rho}_0)_z|^2], \\ \mathcal{B}_{\pm 1} &= \frac{3}{32\pi} [|(\boldsymbol{\rho}_{\pm 1})_x|^2 + |(\boldsymbol{\rho}_{\pm 1})_y|^2 + |(\boldsymbol{\rho}_{\pm 1})_z|^2], \end{aligned} \quad (\text{B1})$$

where $\mathbf{e}_k = \mathbf{k}/k$,

$$\begin{aligned} \boldsymbol{\rho}_0 &= \left(\frac{3(\mathbf{R} \cdot \mathbf{e}_z)\mathbf{R}}{R^2} - \mathbf{e}_z \right) \frac{1 - iR \frac{\omega_A}{c}}{R^3} \\ &\quad - \left(\frac{(\mathbf{R} \cdot \mathbf{e}_z)\mathbf{R}}{R^2} - \mathbf{e}_z \right) \frac{\left(\frac{\omega_A}{c} \right)^2}{R} \end{aligned}$$

and

$$\begin{aligned} \boldsymbol{\rho}_{\pm 1} &= \left(\frac{3(\mathbf{R} \cdot \mathbf{e}_{\pm})\mathbf{R}}{R^2} - \mathbf{e}_{\pm} \right) \frac{1 - iR \frac{\omega_A}{c}}{R^3} \\ &\quad - \left(\frac{(\mathbf{R} \cdot \mathbf{e}_{\pm})\mathbf{R}}{R^2} - \mathbf{e}_{\pm} \right) \frac{\left(\frac{\omega_A}{c} \right)^2}{R} \end{aligned}$$

with $\mathbf{e}_{\pm} = \mathbf{e}_x \pm i\mathbf{e}_y$.

(ii) $\mathcal{A}_{\Delta m}(\mathbf{R}, \Omega_k, \omega_A)$ and $\mathcal{B}_{\Delta m}(\mathbf{R}, \omega_A)$ for the $n_{AP0} \rightarrow \varepsilon_k d$ bound-continuum transition in A and $n_{BS} \rightarrow n'_B p_m$ bound-bound transitions in B :

$$\begin{aligned} \mathcal{A}_0 &= \frac{3}{16} |\mathbf{e}_0 \cdot \boldsymbol{\rho}_0|^2, \\ \mathcal{A}_{\pm 1} &= \frac{3}{32} |\mathbf{e}_0 \cdot \boldsymbol{\rho}_{\pm 1}|^2, \\ \mathcal{B}_0 &= \frac{9}{80\pi} \left[|(\boldsymbol{\rho}_0)_x|^2 + |(\boldsymbol{\rho}_0)_y|^2 + \frac{4}{3} |(\boldsymbol{\rho}_0)_z|^2 \right], \\ \mathcal{B}_{\pm 1} &= \frac{9}{160\pi} \left[|(\boldsymbol{\rho}_{\pm 1})_x|^2 + |(\boldsymbol{\rho}_{\pm 1})_y|^2 + \frac{4}{3} |(\boldsymbol{\rho}_{\pm 1})_z|^2 \right]. \end{aligned} \quad (\text{B2})$$

Here, $\mathbf{e}_0 = 3 \cos \vartheta_k \mathbf{e}_k - \mathbf{e}_z$.

(iii) $\mathcal{A}_{\Delta m}(\mathbf{R}, \Omega_k, \omega_A)$ and $\mathcal{B}_{\Delta m}(\mathbf{R}, \omega_A)$ for the $n_A p_1 \rightarrow \varepsilon_k d$ bound-continuum transition in A and $n_B s \rightarrow n'_B p_m$ bound-bound transitions in B :

$$\begin{aligned} \mathcal{A}_0 &= \frac{3}{2^7} (3 \cos^2 \vartheta_k - 1)^2 |\mathbf{e}_z \cdot \boldsymbol{\rho}_1|^2, \\ \mathcal{A}_{\pm 1} &= \frac{3}{2^8} (3 \cos^2 \vartheta_k - 1)^2 |\mathbf{e}_{\pm} \cdot \boldsymbol{\rho}_{\pm 1}|^2, \\ \mathcal{B}_0 &= \frac{3}{160\pi} \frac{R_z^2 (R_x^2 + R_y^2)}{R^4} \\ &\quad \times \left[\left(\frac{3}{R^3} - \frac{(\frac{\omega_A}{c})^2}{R} \right)^2 + \frac{9(\frac{\omega_A}{c})^2}{R^4} \right], \\ \mathcal{B}_{\pm 1} &= \frac{3}{320\pi} \left[\frac{3}{R^2} (R_x^2 \mp R_y^2 + 2iR_x R_y \delta_{m,1}) \right. \\ &\quad \left. - 2\delta_{m,-1} \right] \frac{1 - iR \frac{\omega_A}{c}}{R^3} \\ &\quad - \left[\frac{1}{R^2} (R_x^2 \mp R_y^2 + 2iR_x R_y \delta_{m,1}) - 2\delta_{m,-1} \right] \left| \frac{(\frac{\omega_A}{c})^2}{R} \right|^2. \end{aligned}$$

(iv) $\mathcal{A}_{\Delta m}(\mathbf{R}, \Omega_k, \omega_A)$ and $\mathcal{B}_{\Delta m}(\mathbf{R}, \omega_A)$ for the $n_A p_{-1} \rightarrow \varepsilon_k d$ bound-continuum transition in A and $n_B s \rightarrow n'_B p_m$ bound-bound transitions in B :

$$\begin{aligned} \mathcal{A}_0 &= \frac{3}{2^7} (3 \cos^2 \vartheta_k - 1)^2 |\mathbf{e}_z \cdot \boldsymbol{\rho}_{-1}|^2, \\ \mathcal{A}_{\pm 1} &= \frac{3}{2^8} (3 \cos^2 \vartheta_k - 1)^2 |\mathbf{e}_{\pm} \cdot \boldsymbol{\rho}_{\pm 1}|^2, \\ \mathcal{B}_0 &= \frac{3}{160\pi} \frac{R_z^2 (R_x^2 + R_y^2)}{R^4} \\ &\quad \times \left[\left(\frac{3}{R^3} - \frac{(\frac{\omega_A}{c})^2}{R} \right)^2 + \frac{9(\frac{\omega_A}{c})^2}{R^4} \right], \\ \mathcal{B}_{\pm 1} &= \frac{3}{320\pi} \left[\frac{3}{R^2} (R_x^2 \pm R_y^2 - 2iR_x R_y \delta_{m,-1}) \right. \\ &\quad \left. - 2\delta_{m,1} \right] \frac{1 - iR \frac{\omega_A}{c}}{R^3} \\ &\quad - \left[\frac{1}{R^2} (R_x^2 \pm R_y^2 - 2iR_x R_y \delta_{m,-1}) - 2\delta_{m,1} \right] \left| \frac{(\frac{\omega_A}{c})^2}{R} \right|^2. \end{aligned}$$

-
- [1] J. Eichler, *Lectures on Ion-Atom Collisions* (Elsevier, Amsterdam, 2005).
- [2] J. Eichler and W. E. Meyerhof, *Relativistic Atomic Collisions* (Academic Press, Cambridge, MA, 1995).
- [3] A. B. Voitkiv, B. Najjari, R. Moshhammer, and J. Ullrich, *Phys. Rev. A* **65**, 032707 (2002); A. B. Voitkiv and B. Najjari, *ibid.* **79**, 022709 (2009).
- [4] Z. Ficek and S. Swain, *Quantum Interference and Coherence* (Springer, Berlin, 2005).
- [5] T. Amthor, M. Reetz-Lamour, S. Westermann, J. Denskat, and M. Weidemüller, *Phys. Rev. Lett.* **98**, 023004 (2007).
- [6] E. A. Jares-Erijman and T. M. Jovin, *Nat. Biotechnol.* **21**, 1387 (2003).
- [7] T. Jahnke, U. Hergenhahn, B. Winter, R. Dörner, U. Fröhling, P. V. Demekhin, K. Gokhberg, L. S. Cederbaum, A. Ehresmann, A. Knie, and A. Dreuw, *Chem. Rev.* **120**, 11295 (2020).
- [8] A. C. LaForge *et al.*, *Sci. Rep.* **4**, 3621 (2014); B. Schütte, M. Arbeiter, T. Fennel, G. Jabbari, A. I. Kuleff, M. J. J. Vrakking, and A. Rouzée, *Nat. Commun.* **6**, 8596 (2015).
- [9] B. Najjari, A. B. Voitkiv, and C. Müller, *Phys. Rev. Lett.* **105**, 153002 (2010); A. B. Voitkiv and B. Najjari, *Phys. Rev. A* **84**, 013415 (2011); A. B. Voitkiv, C. Müller, S. F. Zhang, and X. Ma, *New J. Phys.* **21**, 103010 (2019).
- [10] F. Trinter, J. B. Williams, M. Weller, M. Waitz, M. Pitzer, J. Voigtsberger, C. Schober, G. Kastirke, C. Müller, C. Goihl, P. Burzynski, F. Wiegandt, R. Wallauer, A. Kalinin, L. P. H. Schmidt, M. S. Schöffler, Y. C. Chiang, K. Gokhberg, T. Jahnke, and R. Dörner, *Phys. Rev. Lett.* **111**, 233004 (2013).
- [11] A. Mhamdi, F. Trinter, C. Rauch, M. Weller, J. Rist, M. Waitz, J. Siebert, D. Metz, C. Janke, G. Kastirke, F. Wiegandt, T. Bauer, M. Tia, B. Cunha de Miranda, M. Pitzer, H. Sann, G. Schiwietz, M. Schöffler, M. Simon, K. Gokhberg, R. Dörner, T. Jahnke, and P. V. Demekhin, *Phys. Rev. A* **97**, 053407 (2018).
- [12] A. Hans, P. Schmidt, C. Ozga, C. Richter, H. Otto, X. Holzapfel, G. Hartmann, A. Ehresmann, U. Hergenhahn, and A. Knie, *J. Phys. Chem. Lett.* **10**, 1078 (2019).
- [13] C. Müller, A. B. Voitkiv, J. R. Crespo Lopez-Urrutia, and Z. Harman, *Phys. Rev. Lett.* **104**, 233202 (2010); A. Jacob, C. Müller, and A. B. Voitkiv, *Phys. Rev. A* **100**, 012706 (2019).
- [14] K. Gokhberg and L. S. Cederbaum, *J. Phys. B* **42**, 231001 (2009); A. Jacob, C. Müller, and A. B. Voitkiv, *ibid.* **52**, 225201 (2019).
- [15] F. Grill, A. B. Voitkiv, and C. Müller, *Phys. Rev. A* **100**, 032702 (2019).
- [16] A. B. Voitkiv, *J. Phys. B* **40**, 2885 (2007).
- [17] L. D. Landau and E. M. Lifshitz, *The Classical Theory of Fields* (Pergamon Press, Oxford, 1971); see Sec. 63.
- [18] R. Anholt, *Phys. Rev. A* **19**, 1004 (1979).
- [19] There exist two Li-He dimers, ${}^7\text{Li-He}$ and ${}^6\text{Li-He}$, with the latter being about 4 times weaker bound than the former (5.6 and 1.5 mK, respectively). Since ${}^7\text{Li}$ is much more abundant than ${}^6\text{Li}$, only ${}^7\text{Li-He}$ dimers are considered in this paper.
- [20] N. Tariq, N. Al Taisan, V. Singh, and J. D. Weinstein, *Phys. Rev. Lett.* **110**, 153201 (2013).
- [21] B. Friedrich, *Physics* **6**, 42 (2013).
- [22] Atomic spectra data base of the National Institute of Standards and Technology (NIST), available at <https://www.nist.gov/pml/atomic-spectra-database>.
- [23] D. A. Verner and D. G. Yakovlev, *Astron. Astrophys. Suppl. Ser.* **109**, 125 (1995).
- [24] A. Ben-Asher, A. Landau, L. S. Cederbaum, and N. Moiseyev, *J. Phys. Chem. Lett.* **11**, 6600 (2020).

- [25] J. A. C. Gallas, *Phys. Rev. A* **21**, 1829 (1980).
- [26] F. Grill, A. B. Voitkiv, and C. Müller, *Phys. Rev. A* **102**, 012818 (2020).
- [27] M. Inokuti, *Rev. Mod. Phys.* **43**, 297 (1971).
- [28] J. Berkowitz, *Atomic and Molecular Photoabsorption: Absolute Total Cross Sections* (Academic Press, Cambridge, MA, 2001).
- [29] Y. Kim, J. P. Santos, and F. Parente, *Phys. Rev. A* **62**, 052710 (2000).
- [30] Y. Kim and M. Inokuti, *Phys. Rev.* **175**, 176 (1968).
- [31] M. Inokuti and Y. Kim, *Phys. Rev.* **186**, 100 (1969).
- [32] A. B. Voitkiv and B. Najjari, *Phys. Rev. A* **82**, 052708 (2010).
- [33] L. D. Landau and E. M. Lifshitz, *Quantum Mechanics* (Pergamon Press, Oxford, 1965); see Sec. 19.
- [34] J. R. Swanson and L. Armstrong, Jr., *Phys. Rev. A* **15**, 661 (1977).
- [35] D. J. Kennedy and S. T. Manson, *Phys. Rev. A* **5**, 227 (1972).
- [36] T. N. Chang and T. Olsen, *Phys. Rev. A* **23**, 2394 (1981).